Acta Cardiol Sin 2017;33:630–636
Original Article
doi: 10.6515/ACS20170504A

Cardiovascular Surgery

Surgical Acute Volume-Overload Impacts Early on Myocardium – An Experimental Study

Christa Huuskonen,[1] Mari Hämäläinen,[2] Robin Bolkart,[1] Tatu Soininen,[1] Veera Kähönen,[1] Timo Paavonen,[3] Eeva Moilanen[2] and Ari A. Mennander[1]

Background: Acute volume-overload (AVO) predisposes to cardiac failure. Global cardiac injury may ensue after acute right-sided distension of the heart due to AVO. We experimentally investigated whether surgical AVO impacts early on the myocardium and some markers of injury.

Methods: Thirty-four syngeneic Fisher rats underwent surgical abdominal aortocaval fistula to induce AVO. The hearts were procured for regional and quantitative histology after one and three days. Gene expressions for atrial natriuretic peptide (ANP), matrix metalloprotease 9 (MMP9), transforming growth factor β (TGFβ) and YKL40 were investigated for myocardial injury.

Results: The relative number of ischemic intramyocardial arteries were abundant in the septum of the hearts with AVO compared with controls at day 1 and 3 [0.16 ± 0.02 vs. 0.02 ± 0.01, point score unit (PSU), p = 0.002 and 0.14 ± 0.02 vs. 0.02 ± 0.01, PSU, p = 0.009, respectively] followed by similar changes in the left ventricle at day 3 (0.11 ± 0.02 vs. 0.04 ± 0.01, PSU, p = 0.007). Indicating early myocardial injury, ANP (p = 0.019) was increased in AVO hearts as compared with controls at day 1, as expected. More interestingly, MMP9 (p = 0.003 and p = 0.006), TGFβ (p = 0.002 and p = 0.004) and YKL40 (p = 0.001 and p = 0.003) expressions were significantly increased at day 1 and 3, along with macrophage infiltration into the myocardium supporting the role of factors produced by alternatively activated macrophages in the pathogenesis of AVO-induced pathophysiology in the heart.

Conclusions: Surgical AVO induces an early ischemic myocardial response observed in the intramyocardial arteries. Early expression of key parameters of cardiac remodeling suggest for the onset of early cardiac failure after AVO.

Key Words: Acute volume-overload (AVO) • Myocardial arteries • Rat • YKL40

INTRODUCTION

The presence of acute volume-overload (AVO) and subsequent acute right-sided heart insufficiency are associated with a dismal outcome after cardiac surgery.[1,2] Devastating cardiac entities ensue due to increased cardiac oxygen consumption often despite corrective surgery,[3] and there is increasing awareness of the prognostic significance of right-sided heart congestion during AVO and acute cardiac failure.[4] Low coronary perfusion pressure associated with acute right-sided heart congestion after surgery has been reported to be responsible for early myocardial ischemia, inflammation and cardiac remodeling.[5]

The development of global cardiac injury may ensue upon acute distension of the right side of the heart during AVO. Increased myocardial stretching of the right atrium and ventricle due to AVO may reflect the onset of irreversible cardiac failure. Therefore, it is vital to investigate the early phase of injury associated with AVO after surgery to understand the main pathogenesis re-

Received: December 12, 2016 Accepted: May 4, 2017
[1]Heart Hospital, Tampere University Hospital; [2]The Immunopharmacology Research Group, University of Tampere School of Medicine; [3]Department of Pathology, Fimlab Laboratories, University of Tampere School of Medicine and Tampere University Hospital, Tampere, Finland.
Corresponding author: Dr. Ari A. Mennander, Heart Hospital, Tampere University Hospital, SDSKIR, Teiskontie 35, BOX 2000, 33521 Tampere, Finland. Tel: 358-3-31165048; Fax: 358-3-31165045; E-mail: ari.mennander@sydansairaala.fi

sponsible for irreversible cardiac failure. We hypothesized that surgical AVO induces early ischemic changes in the intramyocardial arteries that nourish the vulnerable myocardium, eventually leading to global cardiac insufficiency.

We developed a rat model simulating AVO induced by surgery by performing a surgical 5-mm long abdominal aortocaval fistula. The aim of this study was to investigate the histology and gene expressions associated with acute myocardial changes after experimental AVO.

MATERIALS AND METHODS

Rats

Thirty-four Fischer 344 rats (F344/NHsd, Harlan Laboratories, The Netherlands) weighing 200-350 g underwent surgical abdominal arterial-venous fistula to induce AVO. In addition, six rats without AVO or surgery served as controls. The rats received humane care in compliance with the "Principles of Laboratory Animal Care" formulated by the National Society for Medical Research and the "Guide for the Care and Use of Laboratory Animals" prepared by the Institute of Laboratory Animal Resources and published by the National Institutes of Health (NIH publication No. 86-23, revised 1996). The study was approved by the State Provincial Office.

Surgical procedure

Rats were anesthetized with sevoflurane (Baxter, USA) via inhalation and pentobarbiturate (Mebunat vet®; Orion Espoo, Finland; 50 mg/kg) intraperitoneally. The abdominal cavity was surgically opened, and the inferior vena cava and aorta were exposed. An arterial-venous fistula was performed intra-abdominally by incising vertically 5 mm both the abdominal aorta and the adjacent inferior vena cava, and joining these vessels surgically with a 7-0 running vascular suture. After surgery, 100 U Heparin Leo, (Vianex S.A., Greece) was administered i.v. From the abdominal aorta, oxygenated blood was introduced into the abdominal vena cava, thus resulting in AVO of the heart. This model allowed us to study the impact of surgically-induced extensive AVO and associated myocardial changes *in-vivo*. The model thus simulated the clinical concept of volume-overload without ischemia but with surgically-induced inflammation. After the procedure, buprenorfin (Vetergesic®; Orion Espoo, Finland; 0.1 mg/100 g) and carprofen (Norocarp®; Norbrook Laboratories Limited, Newry, Northern Ireland; 0.5 mg/100 g) were given subcutaneously for pain relief.

Tissue samples

The rats were sacrificed one (n = 23) or three (n = 7) days after AVO, while four rats were lost due to acute cardiac failure. The basal part of the hearts was separated and stored in RNAlater (Applied Biosystems, CA, USA) for quantitative reverse-transcription polymerase chain reaction (qRT-PCR) analysis. The apex part of the heart was fixed in formalin and embedded in paraffin.

Histology

For histology, 5-μm sections were cut and stained with Hematoxylin and Eosin. The following variables were evaluated from all of the samples: presence of myocardial edema, hemorrhage and ischemia. As vacuolization of nuclei in the media layer of intramyocardial arteries reflects edema, a representative cross-sectional intramyocardial artery was chosen randomly from both the left anterior, septum and right posterior ventricular walls. Normal, vacuolated and sharp-edged media cell nuclei were manually counted separately. The relative number of ischemic nuclei of intramyocardial arteries was calculated by dividing the total number of sharp-edged media cell nuclei by normal round-shaped nuclei. The presence of periadventitial inflammatory cells was graded according to an arbitrary scale from 0 to 1: 0, no inflammation; 1, presence of inflammation. Evaluation of the histology was performed by two investigators (Christa Huuskonen and Robin Bolkart) blinded to the study protocol.

Immunohistochemistry for CD68

Immunohistochemistry was performed using Ventana Lifesciences Benchmark XT © Staining module (Roche Group, Tucson, Arizona, USA). The paraffin-embedded slides were deparaffinized with three changes of xylene, rehydrated in a series of graded ethanol, and rinsed well under running distilled water. The slides were placed in a preheated retrieval buffer containing 0.1 mmol EDTA, pH 8.0, for 30 minutes, then cooled in

the buffer for 5 minutes, followed by a 5-minute rinse under running distilled water. After heat-induced epitope retrieval, the slides were placed on an autostainer (DAKO Corp, Carpinteria, California, USA). The sections were incubated with 3% hydrogen peroxide in ethanol for 5 minutes to inactivate the endogenous peroxides and incubated in CD68 antibody (dilution 1:100) (Biomedica Gruppe, Vienna, Austria) for 30 minutes, followed by rinsing with Tris-buffered saline solution with Tween 20 (TBST) wash buffer. Secondary incubation was performed with DUAL-labeled polymer-horseradish peroxidase (K4061; DAKO Corp) for 15 minutes, and the slides were rinsed with TBST wash buffer. The sections were then incubated in 3,3-diaminobenzidine (K3467, DAKO Corp) for 5 minutes, counterstained with modified Schmidt hematoxylin for 5 minutes, and rinsed for 3 minutes in tap water to blue sections, dehydrated with graded alcohols, and cleared in three changes of xylene before mounting. Positively-stained CD68 deposition was assessed in a representative cross-sectional intramyocardial artery chosen randomly from the left anterior ventricular wall, right ventricular wall and septum. The total amount of myocardial CD68 deposition was calculated accordingly and expressed as PSU. The evaluation was performed by two investigators (Robin Bolkart and Veera Kähönen) blinded to the study protocol.

qRT-PCR analysis

Frozen tissue samples of the base of the heart of six randomly chosen hearts from each group were homogenized and RNA extraction was carried out with a GenElute™ Mammalian Total RNA Miniprep kit (Sigma-Aldrich, St.Louis, MO, USA) with proteinase K treatment. Total RNA was then reverse-transcribed to cDNA using TaqMan® Reverse Transcription reagents and random hexamers (Applied Biosystems, Foster City, CA, USA). The cDNA obtained from the RT reaction (amount corresponding to approximately 1 ng of total RNA) was subjected to quantitative PCR using QuantiTect® Primer Assays (Qiagen, Valencia, CA, USA) for atrial natriuretic peptide (ANP), matrix metalloprotease 9 (MMP9), transforming growth factor β (TGFβ), chitinase 3-like protein (YKL40) and GAPDH, Maxima® SYBR Green/ROX qPCR Master Mix (Thermo Scientific, Waltham, MA, USA), and an ABI PRISM 7000 Sequence detection system (Applied Biosystems, Foster City, CA, USA). The PCR reaction parameters for SYBR® Green detection were as follows: incubation at 50 °C for two minutes, incubation at 95 °C for 10 minutes, and thereafter 40 cycles of denaturation at 95 °C for 15 seconds and annealing and extension at 60 °C for one minute. Each sample was determined in duplicate. Ct values were determined, and the relative quantification was calculated using the $2^{-\Delta\Delta Ct}$ method.[6] We selected a variety of parameters associated with cardiac insufficiency. ANP reflects cardiac insufficiency. MMP9, TGFβ and YKL40 represent tissue remodeling due to ischemia reperfusion injury. The values of six controls were used as a calibrator, and the expression levels of ANP, MMP9, TGFβ and YKL40 were normalized against GAPDH.

Statistical analysis

Data are presented as mean ± standard error of the mean (SEM). Statistical analyses were performed with SPSS statistical software version 22.0 (SPSS Inc., Chicago, IL). Nonparametric data were analyzed between groups using Kruskal-Wallis and Mann-Whitney U tests. A p-value < 0.05 was considered to be statistically significant.

RESULTS

Histology

The absolute numbers of normal, ischemic and vacuolated medial cell nuclei of intramyocardial arteries of the heart with AVO and the controls are shown in Table 1. The absolute number of ischemic nuclei in the intramyocardial arteries was increased in the septum of the hearts with AVO at day one and day three compared with the controls (5.89 ± 1.12 and 5.80 ± 1.07, vs. 0.80 ± 0.37, PSU, p = 0.002 and p = 0.009, respectively, Figure 1). The absolute number of ischemic nuclei in the intramyocardial arteries was also increased in the left ventricle of the hearts with AVO at day three compared with the controls (6.43 ± 1.25, vs. 1.60 ± 0.25, PSU, p = 0.004). There were no significant differences in the presence of subendocardial and myocardial edema, hemorrhage, myocardial inflammation and ischemia of the left and right ventricles between the hearts with AVO and the controls at day one.

As shown in Figure 2, at day one, the relative num-

ber of ischemic nuclei of the intramyocardial arteries was abundant in the septum of the hearts with AVO compared with the controls (0.16 ± 0.02 vs. 0.02 ± 0.01, PSU, p = 0.002), while it did not differ significantly in the right and left ventricles (0.10 ± 0.02 vs. 0.05 ± 0.03, PSU, p = 0.206 and 0.09 ± 0.02 vs. 0.04 ± 0.01, PSU, p = 0.075, respectively). At day three, the relative number of ischemic nuclei of the intramyocardial arteries was increased in the septum and the left ventricle of the hearts with AVO compared with the controls (0.14 ±

Table 1. Histology of media cell nuclei of intramyocardial arteries of the hearts with acute volume-overload (AVO) at one and three days compared with controls

	Controls	AVO day 1	Mann-Whitney U test p-value	AVO day 3	Mann-Whitney U-test p-value	Kruskall-Wallis test p-value
Right ventricle						
Normal nuclei	28.60 ± 3.28	33.09 ± 3.25	0.589	43.00 ± 8.82	0.197	0.206
Ischemic nuclei	1.60 ± 1.03	3.26 ± 0.64	0.170	3.33 ± 0.62	0.153	0.256
Vacuolated nuclei	3.60 ± 1.25	4.48 ± 1.10	0.831	0.67 ± 0.42	0.039	0.057
Left ventricle						
Normal nuclei	42.40 ± 7.31	48.27 ± 3.83	0.435	60.43 ± 4.71	0.166	0.125
Ischemic nuclei	1.60 ± 0.25	4.45 ± 1.09	0.120	6.43 ± 1.25	0.004	0.016
Vacuolated nuclei	6.20 ± 2.15	5.68 ± 2.37	0.208	0.71 ± 0.29	0.012	0.040
Septum						
Normal nuclei	28.60 ± 5.04	38.78 ± 4.54	0.332	43.80 ± 6.83	0.117	0.387
Ischemic nuclei	0.80 ± 0.37	5.89 ± 1.12	0.002	5.80 ± 1.07	0.009	0.008
Vacuolated nuclei	2.80 ± 1.50	5.94 ± 1.54	0.306	0.80 ± 0.37	0.386	0.062

Mann-Whitney U-test and Kruskall-Wallis test p-values. Values are expressed as mean ± standard error of mean.
AVO, acute volume-overload.

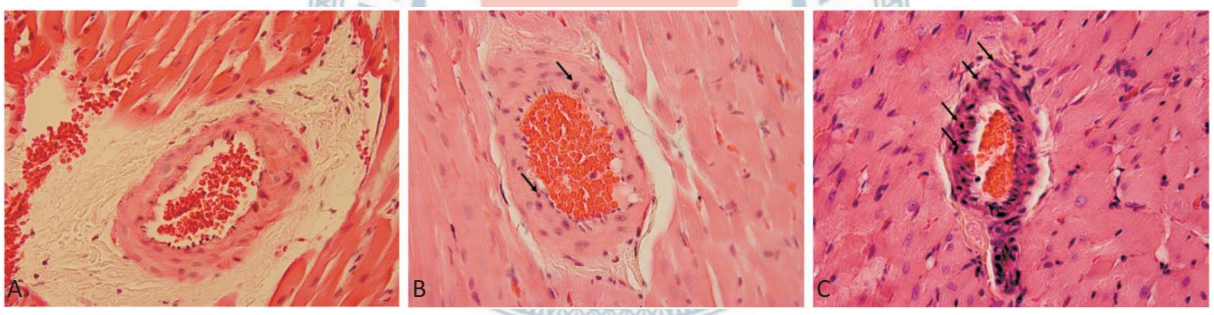

Figure 1. *Representative histology of a septal intramyocardial artery of a heart without AVO (Control; A), and hearts with acute volume-overload one day (AVO 1 day; B) and three days (AVO 3 days; C) after surgery. X40. Note increased dark ischemic nuclei of the media in B and C (arrows).*

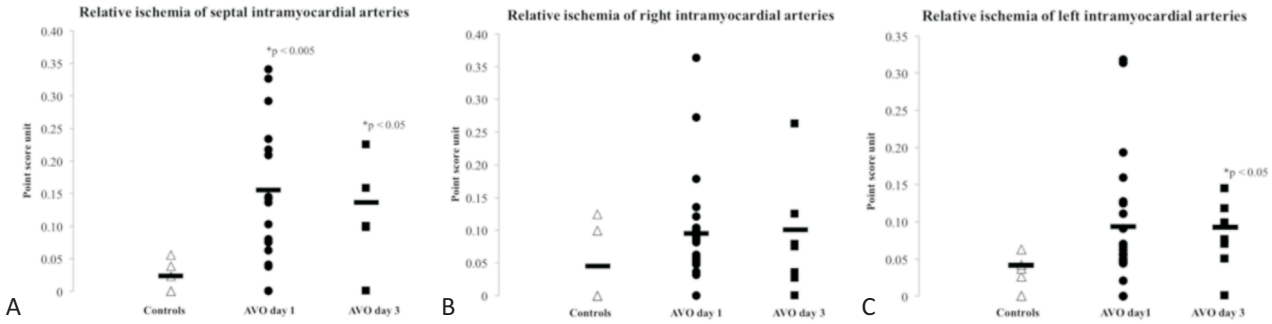

Figure 2. *Relative ischemia of intramyocardial arteries of the septum (A), right ventricle (B) and left ventricle (C) of hearts without AVO (Controls, white triangles), hearts with acute volume overload one day (black circles) and three days after surgery (black boxes). * p < 0.05, Mann-Whitney test. Horizontal bars indicate mean.*

0.02 vs. 0.02 ± 0.01, PSU, p = 0.009 and 0.11 ± 0.02 vs. 0.04 ± 0.01, PSU, p = 0.007, respectively), while it did not differ significantly in the right ventricle (0.10 ± 0.04 vs. 0.05 ± 0.03, PSU, p = 0.230).

Immunohistochemistry for CD68

At day three (Figure 3), the number of CD68-positive cells in the septum was increased in the hearts with AVO compared with the controls (2.33 ± 0.66 vs. 0.20 ± 0.20, PSU, p = 0.027), whereas there were no statistically significant differences in the right or left ventricles between the AVO hearts and the controls (2.83 ± 0.91 vs. 1.00 ± 0.31, PSU, p = 0.135 and 3.83 ± 1.07 vs. 1.20 ± 0.37, PSU, p = 0.079, respectively).

qRT-PCR analysis

At day one, the gene expression of ANP was increased in the hearts with AVO compared with the controls (2.64 ± 0.57 vs. 1.00 ± 0.22, FC, p = 0.019), as expected. Interestingly, the expressions of MMP9, TGFβ and YKL40 were significantly increased in the hearts with AVO both at day one and day three compared with the controls, with YKL40 showing more than a 10-fold increase at day one (Table 2).

DISCUSSION

This study showed that surgical AVO induced acute myocardial ischemia of the right and left ventricles, preceded by septal changes. The absolute number of ischemic nuclei in the intramyocardial arteries were increased initially in the septum, and later, in the left ventricle. Accordingly, the relative number of ischemic nuclei of the intramyocardial arteries were increased first in the septum, and at day three, also in the left ventricle. CD68-positive macrophages were abundant in the septum in the hearts with AVO. All selected gene expressions associated with cardiac insufficiency, including

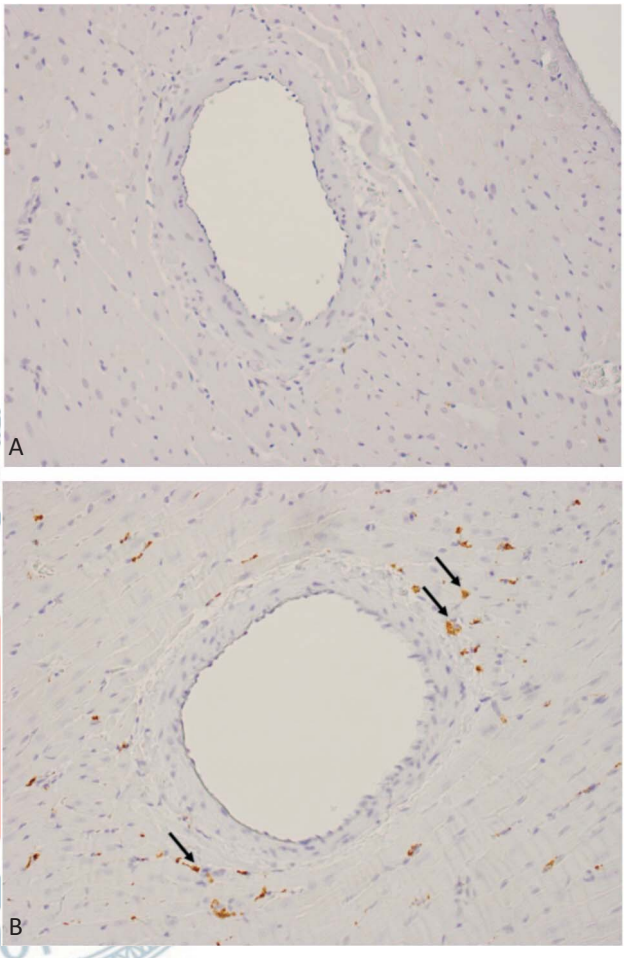

Figure 3. *Representative immunohistochemistry for CD68 deposition of a heart without AVO (Control; A) and a heart with acute volume-overload (AVO; B) three days after surgery. X40. Note positive CD68 staining (arrows) in B associated with periadventitial inflammation of a septal intramyocardial artery.*

Table 2. Gene expression of hearts with AVO at one and three days compared with controls

	Controls	AVO day 1	Mann-Whitney U-test p-value	AVO day 3	Mann-Whitney U-test p-value	Kruskall-Wallis test p-value
ANP	1.00 ± 0.22	2.64 ± 0.57	0.019	2.08 ± 0.66	0.165	0.055
MMP9	1.00 ± 0.39	9.64 ± 2.33	0.003	5.84 ± 1.37	0.006	0.005
TGFβ	1.00 ± 0.12	4.06 ± 0.80	0.002	2.96 ± 0.33	0.004	0.003
YKL40	1.00 ± 0.26	10.79 ± 1.70	0.001	3.91 ± 0.60	0.003	0.001

Values are expressed as mean ± standard error of mean.

ANP, atrial natriuretic peptide; AVO, acute volume-overload; MMP9, matrix metalloproteinase 9; TGFβ, tumor growth factor β; YKL40, chitinase 3-like protein.

ANP, MMP9, TGFβ and YKL40, were increased early after AVO. ANP represents compensation of congestive heart failure due to its vasodilating, antiproliferative, and neurohumoral-modulating capacity.[7] Along with MMP9 and growth factors such as TGFβ, YKL40 expression is a highly promising mediator of tissue remodeling associated with ischemia reperfusion injury.[3,8] Intramyocardial arteries are susceptible to early changes as reflected by increased expressions of parameters associated with the onset of cardiac insufficiency.

Acute right heart dysfunction is an important etiological factor of heart failure after surgery,[1,2] and up to 40% of patients with right ventricle failure experience ongoing right-sided heart volume-overload.[4] Translational research including an animal model of acute right ventricle volume-overload has increased awareness of the molecular mechanisms involved during AVO.[9] In this study, AVO due to surgically-induced aortocaval fistula rendered the myocardium susceptible to acute increased oxygen consumption thus simulating the clinical concept of AVO after surgery; AVO triggered the onset of cardiac remodeling leading to cardiac failure. ANP was increased at day one, indicating that early cardiac failure occurred after AVO. After three days, the acute markers for early heart failure subsided, and an adaptive phase was histologically appreciated as observed by a stabilization of relative ischemia in the septum and both ventricles.

The intramyocardial arteries of the hearts with surgical AVO developed ischemic-like changes including ischemic smooth muscle cell nuclei consistent with sharp-edged dark nuclei. Concomitantly, edematous and vacuolated nuclei were abundant at day one, but decreased significantly at day three. As observed by the relative number of ischemic nuclei of the intramyocardial arteries, the presence of ischemic-like and vacuolated cell nuclei suggests that early changes were subtle in the hearts that already had AVO at day one. Interestingly, the septum seemed to reflect the early volume-overload of the right atrium and ventricle. Indeed, the septum has been shown to be susceptible to acute right-sided heart volume-overload.[10] Early pharmacological interventions could therefore be primarily aimed at preserving the tissue integrity of the septum rather than increasing right-sided cardiac output.

Cardiac inflammation occurs as an early response to acute heart failure.[11] Macrophages, as detected by CD68 immunostaining, infiltrate the periadventitia of the intramyocardial arteries together with the myocardium. Macrophage activity after acute inflammation occurs as a biphasic response changing from the M1 to the M2 macrophage phenotype.[12,13] The pro-inflammatory M1 macrophages give way to the anti-inflammatory M2 macrophages enabling the induction of fibrosis during the proliferative cardiac remodeling phase.[14]

YKL40 contributes to tissue remodeling, although its exact pathogenetic role is still poorly understood.[12,15] YKL40 is a chitinase-like glycoprotein which impacts cell proliferation, differentiation, inflammation, and remodeling of the extracellular matrix.[15] Increased YKL40 and MMP activation has been shown to induce pro-inflammatory and pro-fibrotic cytokines after ischemia-reperfusion injury.[12] In addition, YKL40 regulates the accumulation of T cells and activated macrophages.[15]

Activation of T cells also induces cytokines that regulate TGFβ, and an enhanced TGFβ expression indicates progressive right ventricle volume-overload including septal shift, subendocardial fibrosis and cardiomyocyte apoptosis.[10] Susceptibility to intramyocardial artery edema may be associated with endothelial activity through syndecan-1 and integrins, suggesting the presence of TGFβ and YKL40 activation that leads eventually to tissue fibrogenesis and angiogenesis.[16] The endothelial cell lining of the intramyocardial arteries is the primary target after acute volume-overload upon altered microcirculation of the heart, and therefore markers of endothelial activity such as YKL-40 may be increased. Subsequently, endothelial activity may attract inflammatory cells such as macrophages that interact with MMP9 and TGFβ.

A limitation of this study is that we did not study cardiac function. Creation of a surgical 1.0-1.2-mm long arteriovenous fistula was previously described by Stumpe et al.,[17] and most other models are based on a small aortocaval fistula created by needle puncture.[18] These models are excellent for studying the progression of chronic cardiac failure,[18,19] and demonstration of cardiac function is important to describe these models. Many studies have reported on left-sided ventricle-overload, however this may not be directly extrapolated to congestive heart failure induced by AVO, and different cell signaling pathways and temporal patterns of cardiac re-

modeling may be expected.[18] As clinical scenarios such as AVO have been poorly studied, a significant 5-mm-long arteriovenous fistula was created, and a visual increase in blood flow of the vena cava was evident immediately after suture of the fistula, thus confirming the acute increase in circulating blood flow.

CONCLUSIONS

Volume-overload ultimately leads to the development of eccentric cardiac hypertrophy.[11] Low myocardial perfusion pressure during AVO initiates early left ventricular dysfunction due to acute congestion of the heart and contributes to cardiac remodeling.[5] Taken together, surgical AVO triggers early myocardial ischemia; therefore treatment aimed at protecting intramyocardial arteries may provide a novel strategy against global cardiac detrition after AVO.

DECLARATION OF CONFLICTING INTERESTS

The authors report no conflicts of interest.

REFERENCES

1. Hanai M, Hashimoto K, Mashiko K, et al. Active infective endocarditis. Management and risk analysis of hospital death from 24 years' experience. *Circ J* 2008;72:2062-8.
2. Roberts WC, Shafii AE, Grayburn PA, et al. Clinical and morphologic features of acute, subacute and chronic corpulmonale (pulmonary heart disease). *Am J Cardiol* 2015;115:697-703.
3. Generali T, Garatti A, Biondi A, et al. Aorta to right atrial shunt due to the rupture of a degenerative aneurysm of the noncoronary sinus of Valsalva. *J Cardiovasc Med* 2013;14:71-3.
4. Aronson D, Darawsha W, Atamna A, et al. Pulmonary hypertension, right ventricular function, and clinical outcome in acute decompensated heart failure. *J Cardiac Fail* 2013;19:665-71.
5. Mazzo FR, de Carvalho Frimm C, Moretti AI, et al. Acute aortocaval fistula: role of low perfusion pressure and subendocardial remodeling on left ventricular function. *Int J Exp Pathol* 2013;94:178-87.
6. Livak KJ, Schmittgen TD. Analysis of relative gene expression data using real-time quantitative PCR and the 2-ΔΔCt method. *Methods* 2001;25:402-8.
7. Boerrigter G, Burnett JC. Recent advances in natriuretic peptides in congestive heart failure. *Expert Opin Investig Drugs* 2004;13:643-52.
8. Tiriveedhi V, Upadhya GA, Busch RA, et al. Protective role of bortezomib in steatotic liver ischemia/reperfusion injury through abrogation of MMP activation and YKL-40 expression. *Transpl Immunol* 2014;30:93-8.
9. Reddy S, Zhao M, Hu DQ, et al. Physiologic and molecular characterization of a murine model of right ventricular volume overload. *Am J Physiol Heart Circ Physiol* 2013;304:H1314-27.
10. Buckberg GD, RESTORE Group. The ventricular septum: the lion of right ventricular function, and its impact on right ventricular restoration. *Eur J Cardiothorac Surg* 2006;29:S272-8.
11. Glezeva N, Baugh JA. Role of inflammation in the pathogenesis of heart failure with preserved ejection fraction and its potential as a therapeutic target. *Heart Fail Rev* 2014;19:681-94.
12. Mathiasen AB, Harutyunyan MJ, Jørgensen E, et al. Plasma YKL-40 in relation to the degree of coronary artery disease in patients with stable ischemic heart disease. *Scan J Clin Lab Invest* 2011;71:439-47.
13. Murray PJ, Wynn TA. Protective and pathogenic functions of macrophage subsets. *Nat Rev Immunol* 2011;11:723-37.
14. Riabov V, Gudima A, Wang N, et al. Role of tumor associated macrophages in tumor angiogenesis and lymphangiogenesis. *Front Physiol* 2014;5:1-13.
15. Lee CG, Hartl D, Lee GR, et al. Role of breast regression protein 39 (BRP-39)/chitinase 3-like-1 in Th2 and IL-13-induced tissue responses and apoptosis. *J Exp Med* 2009;206:1149-66.
16. Faibish M, Francescone R, Bentley B, et al. A YKL-40-neutralizing antibody blocks tumor angiogenesis and progression: a potential therapeutic agent in cancers. *Mol Cancer Ther* 2011;10:742-51.
17. Stumpe KO, Sölle H, Klein H, Krück F. Mechanism of sodium and water retention in rats with experimental heart failure. *Kidney Int* 1973;4:309-17.
18. Chen J, Chemaly ER, Liang LF, et al. A new model of congestive heart failure in rats. *Am J Physiol Heart Circ Physiol* 2011;301:H994-1003.
19. Hutchinson KR, Guggilam A, Cismowski MJ, et al. Temporal pattern of left ventricular structural and functional remodeling following reversal of volume overload heart failure. *J Appl Physiol* 2011;111:1778-88.